

Pharmacokinetics of the hypoxia-imaging agent [¹²³I]IAZA in healthy adults following exercise-based cardiac stress

Daria Stypinski¹, Stephen A McQuarrie², Alexander JB McEwan² and Leonard I Wiebe*

Faculty of Pharmacy and Pharmaceutical Sciences, and ²Department of Oncology,
University of Alberta, Edmonton, Canada

Short title: [¹²³I]IAZA pharmacokinetics following cardiac stress

Keywords: scintigraphic imaging, hypoxia, pharmacokinetics, cardiac stress, [¹²³I]IAZA.

¹Current address: Pfizer Inc, San Francisco, USA

*correspondence: Prof. Leonard I Wiebe DSc, PhD, 2-40 Medical Isotope & Cyclotron Facility, 6820 116 St NW, University of Alberta-South Campus, Edmonton, AB T6H 2V8

e-mail: Leonard.wiebe@ualberta.ca

Abstract

Objective: To determine the pharmacokinetics (PK) and detect changes in cardiac uptake of [¹²³I]IAZA, a radiopharmaceutical used to image focal tissue hypoxia, in healthy volunteers after exercise-based cardiac stress, to establish a rational basis for studies of focal myocardial hypoxia in cardiac patients using [¹²³I]IAZA. **Method:** Three healthy male volunteers ran the 'Bruce' treadmill protocol (criterion heart rate is 85 % of [220 – age]). Approximately one minute before reaching this level, [¹²³I]IAZA (4.0 mCi/0.85 mg) was administered as a slow (1-3 min) single bolus i.v. injection, then the volunteer continued running for an additional 1 min. Serum from venous blood samples, taken at pre-determined intervals from 1 min to 45 h, was analyzed by radioHPLC. PK parameters were derived for [¹²³I]IAZA and total radioactivity (total[¹²³I]) using compartmental and noncompartmental analyses (NCA). Whole-body planar scintigraphic images were acquired from 0.75 to 24 h after dosing. PK data and scintigraphic images were compared to published data from healthy volunteers administered [¹²³I]IAZA at rest. **Results:** Following strenuous exercise, both [¹²³I]IAZA and total[¹²³I] exhibited bi-exponential decline profiles, with rapid distribution phases [half-lives ($t_{1/2\alpha}$) of 1.2 and 1.4 min, respectively], followed by slower elimination phases [$t_{1/2\beta}$ of 195 and 290 min, respectively]. Total body clearance (CL_{TB}) and steady state volume of distribution (V_{ss}) were 0.647 L/kg and 185 mL/min, respectively, for [¹²³I]IAZA and 0.785 L/kg and 135 mL/min, respectively, for total[¹²³I]. The $t_{1/2\beta}$, CL_{TB} and V_{ss} values were comparable to those reported previously for rested volunteers. The $t_{1/2\alpha}$ was approximately 4-fold shorter for [¹²³I]IAZA and approximately 3-fold shorter for total[¹²³I] under exercise relative to rested subjects. The heart was visualized in early whole body scintigraphic images, but overall there were no apparent differences from images reported for rested volunteers. Minimal uptake of radiotracer in myocardium and skeletal muscle was consistent with uptake in non-stressed muscle. **Conclusion:** The PK and whole-body scintigrams for [¹²³I]IAZA in exercise-stressed healthy volunteers showed no clinically relevant differences relative to non-exercised volunteers. [¹²³I]IAZA may therefore be suitable for the detection of viable, hypoxic myocardium in areas of myocardial perfusion deficiency.

Keywords: pharmacokinetics, radiotracers, hypoxia, nuclear imaging, [¹²³I]IAZA

Introduction

Nuclear cardiology assesses myocardial viability and establishes a prognosis for cardiac patients [1-3], using a range of radiotracers to observe myocardial perfusion and bioenergetics [4,5]. An alternative imaging approach is to detect pathological, oxygen deficient (hypoxic) myocardial tissue using oxygen-sensitive radiotracers. Radiolabeled azomycins (2-nitroimidazoles such as [¹⁸F]FMISO, [¹⁸F]FAZA, [¹²³I]IAZA, [^{99m}Tc]BMS-181321) and others have been shown to accumulate selectively in hypoxic tissues [6,7]. In theory, these radiotracers concentrate in hypoxic myocardium that has intracellular oxygen partial pressures below about 3 mm Hg (<25 % of normal), and would therefore be useful for assessing myocardial damage. [¹²³I]Iodoazomycin arabinoside ([¹²³I]IAZA) was developed as an imaging agent for the detection of hypoxic, radiation-resistant regions in solid tumors in cancer patients [8-11].

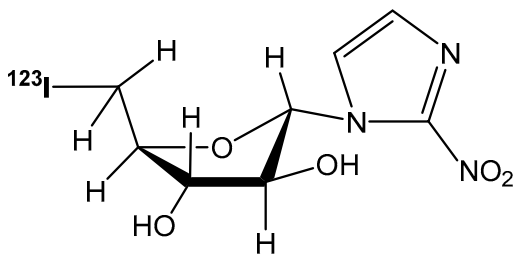


Figure 1. Chemical structure of 1- α -D-(5-deoxy-5-[¹²³I]iodoarabinofuranosyl)-2-nitroimidazole ([¹²³I]iodoazomycin arabinoside; [¹²³I]IAZA).

Its efficacy as a marker of clinical hypoxia in peripheral vascular disease of diabetic origin [12], blunt brain trauma [13] and rheumatoid joints [14], and its clinical pharmacokinetics (PK) and radiation dosimetry in healthy volunteers [15,16] have been reviewed [17].

The first step in determining the suitability of [¹²³I]IAZA as a tool in assessment of myocardial viability in cardiac patients is to establish the impact of physical stress on its baseline PK and chest cavity images. This paper presents [¹²³I]IAZA PK data and planar scintigraphic images for three healthy male volunteers, each of whom received a single i.v. bolus dose of [¹²³I]IAZA while performing strenuous cardiac exercise. These data are compared with previously published results [15, 16] in 6 healthy, rested (no exercise) subjects administered similar [¹²³I]IAZA doses.

Materials and Methods

Clinical and imaging protocols were conducted following the tenets of the Declaration of Helsinki (1964), and were approved by the Alberta Cancer Board Research Ethics Committee (ETH-95-52-19; 1995.10.20; Blood and Urine Sample Analysis and Dosimetry after Intravenous Administration of ^{123}I -IAZA to Volunteers). Three healthy male volunteers (Table 1), aged 27 to 42 years, weighing 70 to 75 kg, participated following informed consent. Lugol's solution (0.6 mL, USP) in orange juice was given orally to block uptake of radioiodide by the thyroid, and shortly thereafter, each volunteer ran the 'Bruce' treadmill protocol. In this test, the criterion heart rate is 85 % of $[220 - \text{age}]$ [18]. Approximately one minute before reaching the target heart rate, each subject received approximately 4.0 mCi/0.85 mg $[^{123}\text{I}]$ IAZA (nominally 185 MBq) as a slow (1-3 min) i.v. bolus injection into a pre-cannulated arm vein. The volunteer then continued running for an additional 1 min.

Pharmacokinetic Analysis (PK): Fourteen venous blood samples (9 mL each) were collected into SST Vacutainer[®] tubes at pre-determined intervals from an indwelling catheter (positioned in the arm contra-lateral to the dosing arm) for analysis of serum $[^{123}\text{I}]$ IAZA and total radioactivity (total $[^{123}\text{I}]$), beginning at pre-dose (0 h) and then post-dose from 1 min to 45 h. Serum samples were analyzed using previously reported serial radiometric high performance liquid chromatography (radioHPLC) [19].

$[^{123}\text{I}]$ IAZA and total $[^{123}\text{I}]$ serum concentrations were analyzed via compartmental and noncompartmental (NCA) methods using WinNonlin version 1.1 (Scientific Consulting Inc). For the compartmental analysis, the choice of model was based on observed and calculated correlation function values, Akaike (AIC) and Schwartz (SC) criteria, and linearity of the partial derivatives plots, with the iteratively reweighted least squares weighing option. Since ^{123}I has a 13.2 h physical decay half-life, instrumental results were decay-corrected for the difference in time from radiometry to the time when the sample was collected.

There is no reported evidence of dose-dependency in $[^{123}\text{I}]$ IAZA PK and hypoxia imaging [15,17]. However, due to variability in individual mass doses of IAZA (Table 1) administered to subjects in the current study (0.57 mg to 1.18 mg, mean of 0.85 mg) and the reference study in rested volunteers, the PK parameters of interest for comparison between the two studies were limited to distribution half-life ($t_{1/2\alpha}$) and elimination half-life ($t_{1/2\beta}$), as

determined using compartmental methods, and steady-state volume of distribution (V_{ss}) and total body clearance (CL_{TB}), determined using NCA.

Imaging: Three SPECT scintigraphs of the chest cavity and five anterior and posterior whole body planar images were acquired at different time periods post injection, beginning immediately after completion of the treadmill protocol (approximately 0.75 h), and at 1-2, 3-4, 6-8 and 20-24 h post injection. All images were acquired over 30 minutes, using a dual-headed, large field of view gamma camera (Picker Odyssey 2000) equipped with a LEAP (low-energy all-purpose) collimator and interfaced to an Odyssey computer. A 20 % analysis window was set symmetrically over the 159 keV I-123 photopeak.

Results

All three subjects who were enrolled in the study completed the protocol with no apparent adverse events. Demographic and dosing information are presented in Table 1.

Pharmacokinetics: The concentration vs time plot for [^{123}I]IAZA and for total [^{123}I] for the three volunteers undergoing the “Bruce” treadmill protocol are shown in Figure 2.

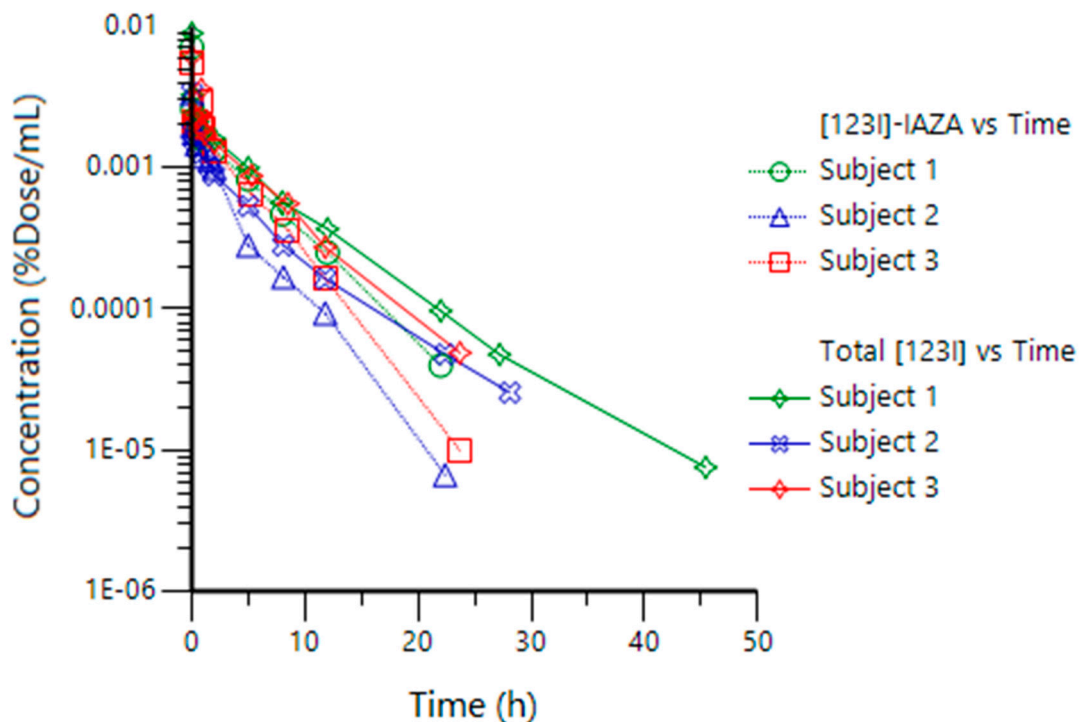


Figure 2. Concentration-time plots for $[^{123}\text{I}]$ IAZA and total $[^{123}\text{I}]$ in each subject.

Both $[^{123}\text{I}]$ IAZA and total $[^{123}\text{I}]$ showed bi-exponential decline profiles following an i.v. bolus dose, with a short and fast distribution phase ($t_{1/2\alpha}$ of 1.2 ± 0.15 and 1.4 ± 0.28 min, respectively), followed by longer elimination phase (195 ± 34 and 290 ± 37 min, respectively). A 2-compartment open model with i.v. bolus input function provided the best fit for the PK data for both $[^{123}\text{I}]$ IAZA and total $[^{123}\text{I}]$ in all subjects, as was the case with rested volunteers [15]. The individual and mean (\pm SD) compartmental ($t_{1/2\alpha}$, $t_{1/2\beta}$), and non-compartmental (V_{ss} and CL_{TB}) PK parameters of interest from the cardiac-stressed volunteers in this study are presented in Table 2, along with comparative historical data for the 6 healthy volunteers dosed under resting conditions [15].

Table 1. Exercise-stressed healthy volunteer demographics and individual IAZA doses. Each subject received a nominal 5 mCi injection of [¹²³I]IAZA. Published data for rested volunteers [15] are included for comparison.

Subject number	Sex	Age (y)	Weight (kg)	Height (cm)	IAZA Dose (mg)
V1	M	42	70	175	0.80
V2	M	27	75	186	1.18
V3	M	40	73	165	0.57
Mean ± SD		36 ± 8	73 ± 3	175 ± 11	0.85 ± 0.31
Reference Study [15]*	4 M 2 F	37 ± 13	80 ± 10	175 ± 9	0.68 ± 0.44

*Mean±SD, N = 6

Table 2. Pharmacokinetic (PK) parameters for [¹²³I]IAZA and total [¹²³I] in exercise-stressed volunteers. Published data for rested volunteers [15] are included for comparison.

PK Subject	[¹²³ I]IAZA				Total [¹²³ I]			
	t _{1/2α} (min)	t _{1/2β} (min)	V _{ss} (L/kg)	CL _{TB} (mL/min)	t _{1/2α} (min)	t _{1/2β} (min)	V _{ss} (L/kg)	CL _{TB} (mL/min)
V1	1.1	234	0.677	145	1.3	328	0.794	104
V2	1.3	170	0.803	254	1.2	287	0.979	182
V3	1.1	182	0.541	157	1.8	254	0.581	120
Exercise*	1.2±0.12	195±34	0.647±0.13	185±60	1.4±0.32	290±37	0.785±0.20	135±41
Rested [15]*	5.3±3.8	179±27	0.716±0.10	239±53	4.6±2.6	294±30	0.746±0.10	145±19

*Mean±SD, N = 6

Imaging: The myocardium and skeletal muscles were only visible in the initial whole body and SPECT images, but not on the later images in this study (Fig. 3). The early, intermediate and late post-dosing whole-body images were consistent with those reported for rested volunteers [16]. On the earliest images, the organs with the highest radioactivity accumulation were the bladder, liver and the kidneys. The i.v. injection site was also visible on the immediate images of one volunteer, but the percent of radioactive dose in that area, as estimated by image inspection, was negligible and therefore not expected to alter the distribution kinetics of the radiopharmaceutical. There was a striking absence of radioactivity in the brains of all the volunteers in early- and intermediate-time images, indicating effective exclusion of $[^{123}\text{I}]$ IAZA by the blood brain barrier. Later images, however, showed some redistribution of radioactivity into the brain. Immediate, 1-2 h and 3-4 h images also did not show thyroid or large intestine uptake, but these organs were visible at late (20-24 h) image acquisition times.

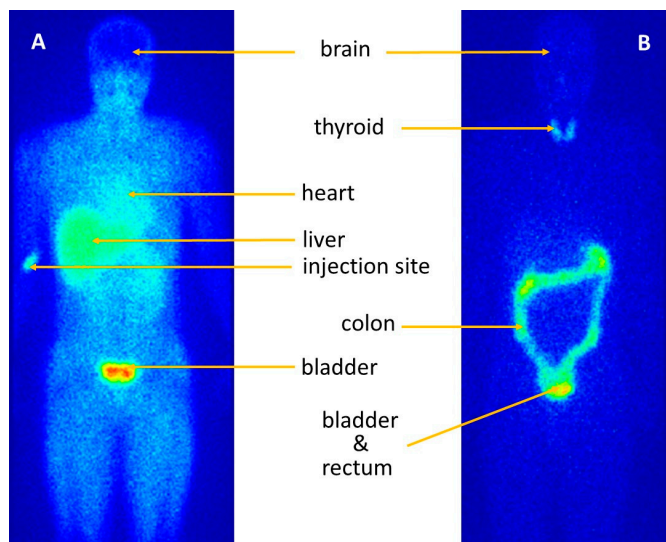


Figure 3. Planar anterior early (A) and late (B) images depicting radioactivity distribution following i.v. injection of $[^{123}\text{I}]$ IAZA in an exercising volunteer. The left image (A), acquired 15 min after injection, shows extensive distribution of radioactivity throughout soft tissues, including viscera, skeletal muscle and heart. The right image (B), acquired 22 h after injection, shows that radioactivity has effectively been cleared from the body except for thyroid and large bowel.

DISCUSSION

Acute strenuous exercise appears to have little impact on the PK of either [¹²³I]IAZA or total[¹²³I] after doses of [¹²³I]IAZA. Only $t_{1/2\alpha}$ was shortened in subjects undergoing the “Bruce” treadmill protocol (1.2 min) relative to rested subjects (5.3 min)[15], which was not unexpected given that strenuous exercise increases both cardiac output and tissue perfusion, hastening drug distribution for lipophilic drugs such as [¹²³I]IAZA. Other PK parameters, $t_{1/2\beta}$, V_{ss} and CL_{TB} , for both [¹²³I]IAZA and total[¹²³I], were comparable between stressed subjects and reference subjects dosed at rest. Since [¹²³I]IAZA distribution is rapid and of short duration, it contributes only approximately 5 % of the overall exposure in subjects at rest [15] and therefore any change in the distribution rate would be expected to have negligible impact on the overall PK profiles of [¹²³I]IAZA and of total radioactivity.

Given the 30 min image acquisition time, the distribution phase is too short to be discernable with gamma camera scintigraphic techniques, a limitation imposed by gamma camera sensitivity and the amount of [¹²³I]IAZA injected. Since the difference in distribution phase could not be captured, the whole-body images obtained from exercising volunteers were consistent with those reported for rested volunteers [16].

The myocardium and the skeletal muscles were visible on the initial whole-body and SPECT images of subjects undergoing exercise; however, all of the whole-body images (early, intermediate and late) were consistent with whole-body images in rested subjects [16]. These results indicate that myocardial radioactivity observed in the early images is most likely attributable to blood pool radioactivity in the heart and in highly perfused cardiac muscle, and not to any stress-induced hypoxia-related retention. This absence of active stress-induced uptake indicates that [¹²³I]IAZA may be suitable for the detection of viable, hypoxic myocardium in areas of myocardial perfusion deficiency.

Accumulation of radioactivity by the large intestine visible on late (20-24 h post-dose) images may be indicative of a minor route of elimination via biliary excretion of radioactivity into the gut. Quantitatively, the amount of radioactivity in the large intestine represented only approximately 5% of the administered dose. Nevertheless, this small amount constitutes a significant relative contribution to the whole-body radioactivity in the late image, given that, as determined from renal excretion of total radioactivity in the 6 healthy volunteers

dosed at rest on the prior study [15], 92% of decay-adjusted total radioactivity was eliminated renally within 28 hours post-dose. However, only approximately 15.5 % of that radioactivity was attributed to intact [^{123}I]IAZA, and therefore the remaining 84.5% was from radiolabeled metabolites, including free [^{123}I]iodide originating via metabolic deiodination of [^{123}I]IAZA. It is possible that some of these metabolites may be excreted into the bile, to be eliminated in feces.

The volunteers in this study received a single oral dose of Lugol's solution immediately before [^{123}I]IAZA injection, to block uptake of [^{123}I]iodide by the thyroid [20]. Quality control during manufacture of the dose assured absence of free [^{123}I]iodide in the injection. However, the thyroid gland, which was barely visible in early images, was clearly present in the late (20 - 24 h) images. Accumulation of radioactivity in the thyroid gland is taken as evidence of metabolic deiodination; in the case of [^{123}I]IAZA, accumulated [^{123}I]iodide represented approximately 0.5% of administered dose. It was concluded that a single dose of cold iodide did not provide a full, lasting blockage, an observation consistent with other reports in the literature [21]. For the exercise study, the radioactivity in the thyroid gland was considered irreversibly bound and eliminated with the 13.2 h decay half-life of the isotope. Since iodine incorporation into the thyroid gland takes place with a 6 - 8 h half-life, it may be possible to further decrease the radiation dose to the thyroid by administering Lugol's solution earlier in the protocol [20,21].

The concentration-time plot of total radioactivity following [^{123}I]IAZA administration exhibits a bi-exponential decline (Fig. 1), and therefore only two compartments were discernible. However, gamma camera scintigraphic images of the whole body delineate several physiological regions with elevated radioactivity, including liver, kidney and thyroid. Radiopharmaceutical imaging is therefore a natural element of physiologically based pharmacokinetic (PBPK) modelling. PBPK can be used to assess the exposure in a target organ after dosing, taking into account organ-specific absorption, metabolism and disposition rates in that organ [22]; it does not rely heavily on plasma or serum PK to elucidate all of the physiological compartments. In the current imaging work, attempts to discern whether these regions are separate compartments of a multicompartmental pharmacokinetic model for [^{123}I]IAZA were unsuccessful, given that scintigraphic images reflect total radioactivity and

[¹²³I]IAZA is known to be extensively metabolized. For example, the thyroid represents less than 0.5% of the all body cumulated activity; however, all of it is attributable to free [¹²³I]iodide, and therefore would not constitute a distinct compartment in a physiologically based PK model for [¹²³I]IAZA. The critical limitation for the use of imaging techniques to aid PBPK modeling is that scintigraphic imaging ‘sees’ all radioactivity regardless of its chemical form – for example on this study the gamma camera was imaging total [¹²³I] disposition; not only [¹²³I]IAZA but [¹²³I]IAZA plus all its radiolabeled metabolites. .

Conclusion

Data from this study support the conclusion that acute strenuous exercise has little or no impact on the PK of either [¹²³I]IAZA or total [¹²³I]. There were no observed differences between scintigraphic images of exercising and resting volunteers. The absence of active stress-induced uptake indicates that [¹²³I]IAZA may be suitable for the detection of viable, hypoxic myocardium in areas of myocardial perfusion deficiency.

Acknowledgements

IAZA was synthesized by Dr. Elena Atrazheva (Faculty of Pharmacy and Pharmaceutical Sciences, University of Alberta) and Ronald P Schmidt (Cross Cancer Institute, Edmonton) provided [¹²³I]IAZA for these studies. This research was supported in part through grant RI-14, Alberta Cancer Board.

References

- [1] Travin, M.I.; Bergmann, S.R. Assessment of myocardial viability. *Sem Nucl Med* **2005**, 35, 2-16, doi: <http://dx.doi.org/10.1053/j.semnuclmed.2004.09.001>.
- [2] Peterson, L.R.; Gropler, R.J. Radionuclide Imaging of Myocardial Metabolism. *Circulation: Cardiovascular Imaging* **2010**, 3, 11-22, doi.org/10.1161/CIRCIMAGING.109.860593.
- [3] Husain, S.S. Myocardial perfusion imaging protocols: Is there an ideal protocol? *J Nucl Med Technol* **2007**, 35, 3-9, PMID:17337651.
- [4] Lawal, I.; Sathekge, M. F-18 FDG PET/CT imaging of cardiac and vascular inflammation and infection. *Brit Med Bull* **2016**, 1-20, doi: 10.1093/bmb/lbw035.

[5] Mather, K.J; DeGrado, T.J. Imaging of myocardial fatty acid oxidation. *Biochim Biophys Acta (BBA) - Molecular and Cell Biology of Lipids* **2016**, 1861, 1535-1543, doi.org/10.1016/j.bbalip.2016.02.019.

[6] Kumar, P.; Bacchu, V.; Wiebe, L.I. The chemistry and radiochemistry of hypoxia-specific, radiohalogenated nitroaromatic imaging probes. *Semin Nucl Med* **2015**, 45, 122-135 C, doi: 10.1053/j.semnuclmed.2014.10.005.

[7] Ricardo, C.L.; Kumar, P.; Wiebe, L.I. Bifunctional metal - nitroimidazole complexes for hypoxia theranosis in cancer. *J Diag Imag Therapy* **2015**, 2, 103-158, doi: http://dx.doi.org/10.17229/jdit.2015-0415-015.

[8] Mannan, R.H.; Somayaji, V.V.; Lee, J.; Mercer, J.R.; Chapman, J.D.; Wiebe, L.I. Radioiodinated 1-(5-iodo-5-deoxy- β -D-arabinofuranosyl)-2-nitroimidazole (iodoazomycin arabinoside: IAZA), a novel marker of tissue hypoxia. *J Nucl Med* **1991**, 32, 1764-1770, PMID:1880579.

[9] Parliament, M.B.; Chapman, J.D.; Urtasun, R.C.; McEwan, J.B.; Golberg, L.; Mercer, J.R.; Mannan, R.H.; Wiebe, L.I. Non-invasive assessment of human tumour hypoxia with ^{123}I -iodoazomycin arabinoside: Preliminary report of a clinical study. *Br J Radiol* **1991**, 65, 90-95, PMC1977349.

[10] Groshar, D.; McEwan, A.J.B.; Parliament, M.B.; Urtasun, R.C.; Golberg, L.E.; Hoskinson, M.; Mercer, J.R.; Mannan, R.H.; Wiebe, L.I.; Chapman, J.D. Imaging tumor hypoxia and tumor perfusion. *J Nucl Med* **1993**, 34, 885-888, PubMed: [8389842](#).

[11] Urtasun, R.C.; Parliament, M.B.; McEwan, A.J.; Mercer, J.R.; Mannan, R.H.; Wiebe, L.I.; Morin, C.; Chapman, J.D. Measurement of hypoxia in human tumours by non-invasive SPECT imaging of azomycin arabinoside. *Br J Cancer* **1996**, 74, S209-S212, PMID:8763882.

[12] Al-Arafaj, A.; Ryan, E.A.; Hutchinson, K.; Mannan, R.H.; Mercer, J.; Wiebe, L.I.; McEwan, A.J.B. An evaluation of ^{123}I -iodoazomycin arabinoside ($[^{123}\text{I}]\text{-IAZA}$) as a marker of localized tissue hypoxia in patients with diabetes mellitus. *Eur J Nucl Med* **1994**, 21, 1338-1442, doi.org/10.1007/BF02426699.

[13] Vinjamuri, S.; O'Driscol, K.; Maltby, P.; McEwan, A.J.; Wiebe, L.I.; Critchley, M. Identification of hypoxic regions in traumatic brain injury. *Clin Nucl Med* **1999**, 24, 891-892, PMID:10551478.

[14] McEwan, A.J.B.; Skeith, K.J.; Mannan, R.H.; Davies, N.; Jamali, F.; Schmidt, R.;

Golberg, K.; Wiebe, L.I. Iodine-123 iodoazomycin arabinoside (IAZA) may have a role in imaging rheumatoid arthritis [abstract]. *J Nucl Med* **1997**, *38* (suppl), 300-301.

[15] Stypinski, D.; Wiebe, L.I.; McEwan, L.I.; Schmidt, R.P.; Tam, Y.K.; Mercer, J.R. Clinical pharmacokinetics of ¹²³IAZA in healthy volunteers. *Nucl Med Commun* **1999**, *20*, 559-567, PubMed:10451869.

[16] Stypinski, D.; McQuarrie, S.A.; Wiebe, L.I.; Tam, Y.K.; Mercer, J.R.; McEwan, A.J.B. Pharmacokinetic validation of scintigraphic dosimetry estimations for ¹²³I-IAZA in healthy subjects. *J Nucl Med* **2001**, *42*, 1418-1423, doi:

[17] Wiebe, L.I.; McEwan, A.J.B. Scintigraphic imaging of focal hypoxic tissue: Development and clinical applications of ¹²³I-IAZA. *Brazilian Arch Biol Technol* **2002**, *45*, S89-102, doi.org/10.1590/S1516-89132002000500010.

[18] Bruce, R.A. Multi-stage treadmill test of maximal and sub maximal exercise. In: AHA: Exercise Testing and Training of apparently Health Individuals: A handbook for physicians. New York **1972**.

[19] Stypinski, D.; Wiebe, L.I.; Mercer, J.R. A rapid and simple assay to determine the blood and urine concentrations of 1-(5-[^{123/125}I]iodo-5-deoxyarabinofuranosyl)-2-nitroimidazole, a hypoxic cell marker. *J Pharm Biomed Analysis* **1997**, *16*, 1067-1073, doi.org/10.1016/S0731-7085(97)00125-8.

[20] Reiners, C.; Schneider, R. Potassium iodide (KI) to block the thyroid from exposure to I-131: current questions and answers to be discussed. *Radiat Environ Biophys* **2013**, *52*, 189-193, doi.org/10.1007/s00411-013-0462-0.

[21] Cavina, L., van der Born, D.; Klaren, P.H.M.; Feiters, M.C.; Boerman, O.C.; Rutjes, F.P.J.T. Design of radioiodinated pharmaceuticals: structural features affecting metabolic stability towards in vivo deiodination. *Eur J Org Chem* **2017**, 3387-3414, doi:10.1002/ejoc.201601638.

[22] Zhuang, X.; Lu, C. PBPK modeling and simulation in drug research and development. *Acta Pharmaceutica Sinica B* **6**, *2016*, 430-440, doi.org/10.1016/j.apsb.2016.04.004